water

MDPI

Article

Phosphorus Recovery and Simultaneous Heavy Metal Removal from ISSA in a Two-Compartment Cell

Le Fang [1,*], Zuotai Zhang [2,*], Ying Mei [1], Linji Xu [3] and Ze Ren [1]

[1] RDC for Watershed Environmental Eco-Engineering, Advanced Institute of Natural Sciences, Beijing Normal University at Zhuhai, No. 18 Jinfeng Road, Xiangzhou District, Zhuhai 519080, China
[2] Guangdong Provincial Key Laboratory of Soil and Groundwater Pollution Control, Southern University of Science and Technology, Shenzhen 518055, China
[3] Faculty of Environment and Ecology, Chongqing University, Chongqing 400044, China
* Correspondence: fang.le@bnu.edu.cn (L.F.); zhangzt@sustech.edu.cn (Z.Z.)

Abstract: Traditional acid extraction or electrodialytic remediation (EDR) is inefficient to recover phosphorus (P) from incinerated sewage sludge ash (ISSA). This study used a hybrid process including acid extraction and EDR to extract P from ISSA and remove heavy metals/metals from the P extract sequentially. Specifically, the P extract was obtained by extracting ISSA with 0.2 M H_2SO_4 and a two-compartment cell was applied in the following EDR process. Constant currents of 15 mA, 35 mA and 50 mA were applied for the electromigration of the heavy metals/metals. Results showed that the efficiency of heavy metals/metals removal fluctuated and was relatively low (approximately 20%) under a current of 15 mA. Increasing the current to 35 mA significantly increased the removal efficiency and that of 50 mA was conspicuous, except Fe, Al and As (<50%). Meanwhile, P gradually immigrated to the catholyte after an EDR duration of 96 h. Consistent with heavy metal/metal immigration results, the pH change and 50 mA voltage drop were dramatic (the pH change was 12 and the voltage drop was 11 V). In addition, flocculent precipitates, which were predominantly Ca, P, Al, Mg and Fe, were found in the catholyte.

Keywords: electrodialytic remediation; phosphorus recovery; removal of heavy metals; incinerated sewage sludge ash; two-compartment cell

Citation: Fang, L.; Zhang, Z.; Mei, Y.; Xu, L.; Ren, Z. Phosphorus Recovery and Simultaneous Heavy Metal Removal from ISSA in a Two-Compartment Cell. *Water* **2023**, *15*, 226. https://doi.org/10.3390/w15020226

Academic Editors: Laura Bulgariu and Andrea G. Capodaglio

Received: 29 November 2022
Revised: 30 December 2022
Accepted: 30 December 2022
Published: 4 January 2023

1. Introduction

Phosphorus (P)-containing wastes pose potential risks to the environment; thus, properly recovering P from wastes would prevent pollution and decrease the pressure of P resource shortages. Incinerated sewage sludge ash (ISSA) is a high socioeconomic value P-containing waste that is increasingly produced from sewage sludge incineration plants [1]. Previous researchers used several methods to recover P from ISSA, such as thermal treatment, wet extraction and electrodialytic remediation (EDR) [2–4]. Thermal methods use chlorides as additives to evaporate metals at high temperatures (1000 °C) but nonvolatile metals (such as Ni and Cr) remain [5–7]. During wet extraction, acids are applied to extract P from ISSA but the co-dissolution of metals causes another purification problem [8,9]. EDR applies a current to cause the electromigration of metal(loid)s from the anolyte to the catholyte and segregates by a cation exchange membrane, but the clog of the membrane decreases the recovery efficiency and the duration is normally long (approximately 14 days) [10–12]. For these three kinds of methods, the P phases and heavy metal species determine the P recovery efficiency; thus, many researchers tried to stabilize the heavy metals in ISSA and increase the P availability of recovered substances. Additives such as chlorides, sulfates, carbonates, sand and organic wastes were added to sewage sludge before incineration in order to alter the leachability of P and heavy metals [13,14]. In addition, different extractants, extraction conditions and selective adsorbents were used to

obtain higher P purity and plant-available recovered substances [15,16]. However, these purification methods bring other problems, such as the regeneration of adsorbents.

The EDR was first contrived at the Technical University of Denmark in 1992 and patented in 1995 (PCT/DK95/00209) [17]. EDR is an electrochemical method that not only can separate impurities from liquids, but also can recover valuable metals [18–21]. With continual electric input, the phosphate anion is retained in the anolyte and H^+ is released from water splitting and formed with H_3PO_4 [12]. Meanwhile, the positively charged heavy metal/metal ions migrate to the cathode and are retained by membrane. Aji et al. (2012) used EDR, assisting with monopolar iron electrodes to remove heavy metals (Cu, Zn, Ni and Mn) from wastewater [22]. Wang et al. (2003) studied the effect of EDR on the removal of arsenic by co-precipitation with iron hydroxide [23]. Cr (VI) was removed from aqueous solutions by a process of electrodialysis with liquid membranes [24]. However, these studies directly add sediment or ashes in anolyte, aiming to remove heavy metals by electromigration, which requires extra stirring set-up and long acidification period. The energy distribution analysis identified that the transport of ionic species through the soil suspension consumed the most energy, followed with membranes and electrolytes [17,25]. Therefore, to save energy and simplify processing set-up, more studies that focus on heavy metal/metal electromigration in complex reagents to recover valuable resources are necessary.

To effectively obtain highly purified P extract with relatively low energy consumption, this study combined the advantages of wet extraction and EDR. Specifically, P extract was obtained by a sulfuric acid extraction of ISSA under optimized conditions, which have been examined in a previous study, and then by purification of the P extract by EDR [9]. A two-compartment setup was applied in EDR because of its shorter acidification process, high clean-up level and lower energy consumption [10,26]. A cation exchange membrane was placed in between the cathode and anode, which only allows the migration of positively charged metal(loid)s to occur from the anode to the cathode. The electromigration of metals/heavy metals (Al, Fe, Mn, Pb, Zn, Ni, Cu, Cd and Cr) between electrolytes was studied. Metals, including Al, Fe and Mn, were given special consideration because they co-precipitated with P preferentially, which hampered the precipitation of the desired P product (such as CaH_2PO_4).

The acid retreatment of ISSA can dramatically shorten the acidification and desorption process, afford stable conductivity liquids and prevent the congestion problem in cation exchange membranes [27,28]. Comparatively, a long duration (>7 d) is necessary for the direct EDR of ISSA to release P and the heavy metals that are simultaneously extracted from ISSA, which requires considerable energy and treatment times [17,18,29]. The EDR process can remove heavy metals/metals to a certain degree and obtain a purified P extract, which can be recovered with high-purity P precipitates (such as aluminum hydroxyphosphate) by pH adjusting to 4 and avoiding the co-precipitation of heavy metals/metals [30,31]. With P purification from the acid extract of ISSA as the final goal, this study generally aimed at achieving the (i) electromigration of heavy metals/metals from the acid extract of ISSA and, if possible, (ii) obtaining purified P extract in anolytes and heavy metal/metal hydroxides in catholyte.

2. Experimental Process

2.1. P Extract from ISSA

The ISSA was collected from the Hong Kong T·park (Tuen Men in Hong Kong, China), which was produced by incinerating sewage sludge at 850 °C for 2 s. This ISSA was characterized in our previous findings [9]. In this study, the P extract was obtained by 0.2 M H_2SO_4 with a liquid-to-solid ratio of 20:1 for 4 h, and then centrifuged and filtered through a 0.45 μm mixed cellular filter (Jinteng, Shanxi, China), as in our previous study [9]. The physical and chemical characteristics of the P extract are shown in Table 1. All the reagents used in this study were of analytical grade.

Table 1. Physical and chemical characteristics and heavy metal content in the P extract of the ISSA.

P Extract	pH	Concentration of Major Metal(loid)s (mg/L)	Concentration of Minor Metal(loid)s (μg/L)
Sulfuric acid extract of the ISSA	1.5	Ca (2068), P (1792), Al (1309), Mg (6), Fe (4.6), Zn (0.7), Cu (0.3), Mn (0.16).	As (10.6), Ni (10.8), Pb (10.2).

2.2. EDR Experiments

As illustrated in Figure 1, the cation exchange membrane (CEM, CMI 7000, Membranes International Inc. 219, Margaret King Avenue Ringwood, NJ 07456.) was located between two Plexiglas tanks with an internal capacity of 240 mL (8 × 6 × 5 cm^3). The obtained P extract of ISSA was used as anolyte (200 mL), while the 0.01 M $NaNO_3$ was used as the catholyte with the same volume. The initial pH of the catholyte was adjusted to 1.5, which was the same as that of the anolyte. Two EDR processes applied constant electric currents of 15 mA, 35 mA and 50 mA, whose current densities were corresponding to 0.5 mA/cm^2, 1.17 mA/cm^2, and 1.67 mA/cm^2. The voltage changes between the two electrodes were recorded by an electrochemical workstation (CS 2350, Wuhan Kost Co., Wuhan, China). Platinum-coated electrodes (1 × 1 cm^2) were placed separately in two compartments (anode and cathode). Simultaneously, the variations in pH for the anolyte and catholyte were measured by a pH meter. The electromigration of metal(loid)s and P was evaluated by sampling 1 mL of anolyte/catholyte every time interval. Prior to sampling, the anolyte was stirred to obtain uniformity, and some HNO_3 was added to the collected samples to prevent precipitation. The concentrations of heavy metals/metals were evaluated by ICP–OES (FMX 36, SpectroBlue, Kleve, Germany). In addition, the concentration of P was tested by measuring the absorbance of a developing "molybdenum blue" at 882 nm in a spectrophotometer, as performed in a previous study [9].

In the EDR process, the current assists the electromigration of positively charged heavy metals/metals from the anolyte to the catholyte, thus purifying the P extract. The removal efficiencies of heavy metals/metals were determined as follows:

- The reduction efficiency was calculated from the decrease in heavy metals/metals in the anolyte and verified from the increase in heavy metals/metals in the catholyte. The acceptable mass balances were set in the range of 90–110%.
- The total volume decrease in electrodes was considered when the EDR duration was higher than 96 h.
- An analysis of variance was run for each element and sample, and each of these currents was carried out twice for trend line rectification. The overall results were shown in one trend line.

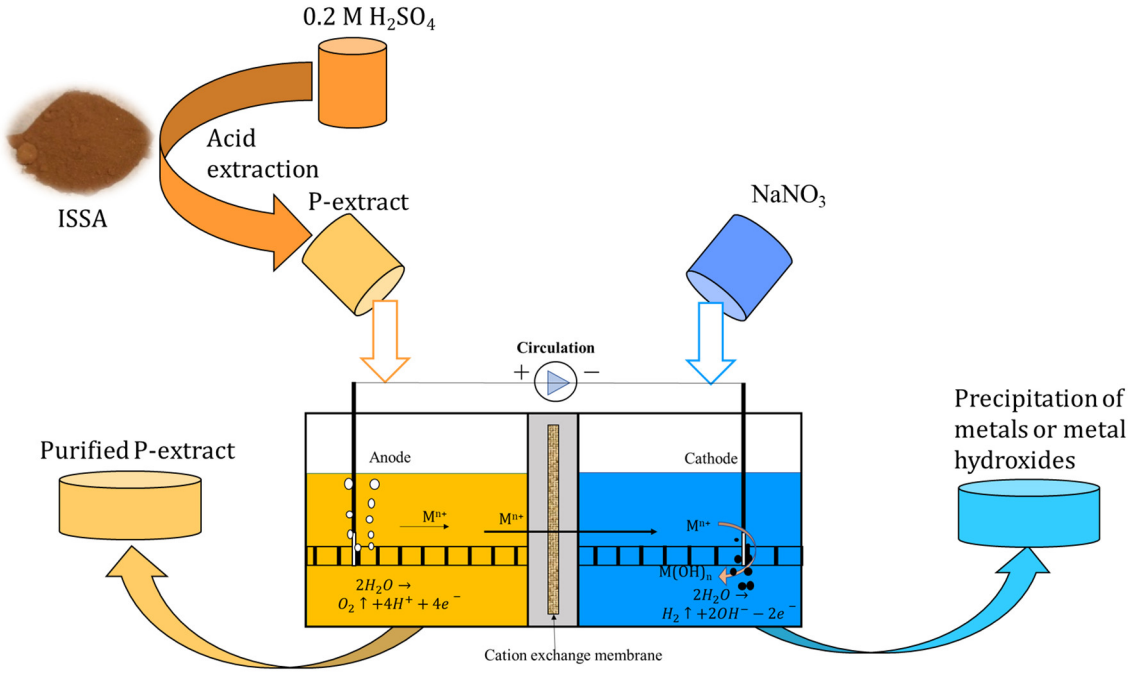

Figure 1. Schematic process of the electrodialytic process.

2.3. Migration of Metal(loid)s and P in Electrolytes

The charge of metal(loid)s and P determines their electromigration in the anolyte and catholyte. To study the existing form of metal(loid)s, Visual MINTEQ 3.1 was used to calculate their concentration and Log K of different aqueous species, as shown in Table 2.

Table 2. Aqueous species of the major metal(loid)s in the extract.

Metal(loid)s	Aqueous Species	Concentration (mmol/L)	Log K
Ca	Ca^{2+}	33.71	−2.01
	$CaSO_4$	16.48	−1.75
	CaH_2PO_4+	1.16	−3.07
Al	$AlSO_4^+$	29.46	−1.67
	$Al(SO_4)^{2-}$	12.47	−2.04
	Al^{3+}	6.57	−3.39
Mg	Mg^{2+}	0.25	−4.15
Fe	$FeH_2PO_4^{2+}$	0.04	−4.93
	$FeSO_4^+$	0.03	−4.66
	$Fe(SO_4)^{2-}$	3×10^{-3}	−5.65
	Fe^{3+}	2.6×10^{-3}	−6.8
Zn	Zn^{2+}	3×10^{-3}	−5.53
Cu	Cu^{2+}	5×10^{-3}	−5.88
Mn	Mn^{2+}	3×10^{-3}	−6.08
Pb	Pb^{2+}	4.8×10^{-5}	−7.87
	$PbH_2PO_4^+$	2.3×10^{-6}	−6.78
As	H_3AsO_3	1.4×10^{-4}	−6.81

For the repeatability of the EDR process, the mass balances of heavy metals, metals and P were calculated for verification during the process. The energy consumption of the EDR process was calculated by the following equation:

$$W = \int U \times IT \quad (1)$$

W is the consumed energy (kw.h), U is the voltage between electrodes (v) and T is the EDR time (h).

2.4. Characterization of the Precipitates in the Cathode

After the EDR process, two kinds of precipitates (precipitate 1, yellow color; precipitate 2, white color) in the catholyte were separately collected and oven-dried at 102 °C for further characterization. To detect the crystalline phases of the precipitates, X-ray diffraction (XRD, Rigaku Smart LAB, Tokyo, Japan) was applied in the 2θ range of 10–90°, with a scanning increment of 0.02° at 2 s per step. In addition, the microstructure and element mapping of the precipitates were evaluated by a field emission scanning electron microscope (SEM, Zeiss, Merlin, Germany).

The surface organic functional groups in the samples were characterized by Fourier transform infrared (FTIR) spectroscopy. The samples were ground and mixed with KBr to 0.1 wt.%, and then pressed into pellets. The spectra of the samples were measured by a Nicolet Nexus 410 and recorded in the range of 4000–400 cm^{-1}. Scanning electron microscopy connected to energy-dispersive spectrometry (SEM-EDX, Tescan Mira 3, Czech Republic) was conducted for morphological and qualitative analyses of the chemical composition of precipitates.

3. Results and Discussion

3.1. Electromigration of Heavy Metals/Metals

The P extract of ISSA was highly acidic and dominantly contained Ca (2068 mg/L), P (1792 mg/L) and Al (1309 mg/L), as shown in Table 1.

The response priority of metals (Ca, Fe, Al, Mn and Mg) and heavy metals (Cd, Pb, Zn, Cu and Ni) under two current intensities was compared by their concentration changes in the anolyte in the first 4 h, as shown in Figure 2. For a current of 15 mA, only partial Ca tended to the anolyte. Increasing the current to 35 mA, the response priority of heavy metals/metals was in the sequence of Cd > Pb ≈ Mg > Zn ≈ Ca > Mn ≈ Ni > Cu > Al. Marginal Fe was decreased in the anolyte and, thus, is not shown in the figure. Increasing the current intensity to 50 mA enhances the electromigration of cations, as expected, especially for Ca, Pb, Cu and Ni. The overall heavy metal/metal removal efficiency in the first 4 h was approximately 77%. The response priority sequence of 50 mA was changed to Ca > Pb ≈ Cd > Mg > Zn > Ni ≈ Cu > Mn > Al.

The electromigration of heavy metals/metals was impelled by the charge and limited by the size of different heavy metal/metal forms; hence, the heavy metal/metal species of P extract were estimated by Visual Minteq (Table 2) [32]. As shown, Ca, Mg, Zn, Cu, Mn and Pb were dominantly in divalent forms. The Al was mainly in the form of $AlSO_4$+ and $Al(SO_4)^{2-}$, while the Fe was primarily in the form of $FeH_2PO_4^{2+}$, $FeSO_4^{+}$ and $Fe(SO_4)^{2-}$. In addition, As was mainly in the form of a molecule (H_3AsO_3). Thus, the low immobilization of Al, Fe and As could be due to their lower charge and relatively larger steric-hindrance effect due to their hydrated ionic radius, which is larger compared with that of other cations [33]. Therefore, it can be predicted that even prolonging the EDR process does not significantly promote the removal efficiencies of Fe, Al and As. Instead, membrane modification, such as tailoring membranes with larger ionic transport channels and, thus, higher water uptake, might be a preferable method for concentrating Fe, Al and As in catholytes [34]. Although a membrane with better ionic permeability generally compromises its selectivity due to the cation mobility that is simultaneously enhanced, such changes in membrane performance are acceptable in this study.

In addition, the variations in P concentration of these three currents are compared in Figure 2d. The P concentration in anolyte under 15 mA is relatively stable, while that

under 50 mA shows a slight increase. There is a P concentration drop between 1 and 2 h at 35 mA (Figure 2), which may be due to P combining with heavy metal cations and transferring into anolyte [11,17]. The subsequent increase in the P concentration is related to the released free H^+ in the anolyte by water electrolysis, which transfers the precipitates to dissolved species (such as PbH_2PO_4). At a current of 50 mA, the P concentration continually increased due to the release of H^+, which is faster than that at a 35 mA current. These P concentration variation results are consistent with pH results in Figure 2e. As shown, the fastest pH drop is found under a current of 50 mA due to water splitting. This observation can be further validated by considering the more acidic anolyte at 50 mA, in which the proton production rate obviously outweighs the rate of proton transport from the anolyte towards the catholyte. Consistently, the variation changes in P concentration explained the fluctuation of heavy metal/metal removal efficiency in the EDR process.

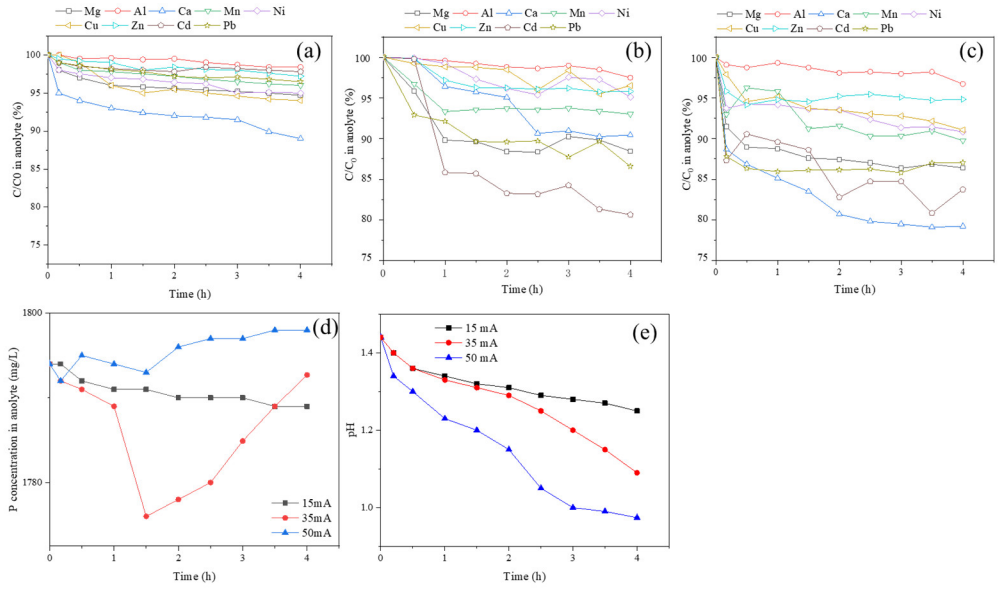

Figure 2. Heavy metals/metals (C/C_0 in percentage) ((**a**–**c**) is 15 mA, 35 mA and 50 mA, respectively), P concentration (**d**) and pH changes (**e**) in anolyte, in first 4 h.

3.2. Optimal Duration of the EDR Process for Heavy Metal/Metal Removal

In the longer EDR process, the pH in the anolyte and catholyte are significantly influenced by the half reactions at the electrodes, as follows:

$$\text{Anode: } 2H_2O \rightarrow O_2(g) + 4H^+ + 4e^- \quad (2)$$

$$\text{Cathode: } 4H_2O + 4e^- \rightarrow 2H_2(g) + 4OH^- \quad (3)$$

Thus, the pH of the anolyte and catholyte exhibits opposite changes with the operation of the EDR process, which determines the heavy metals/metals and P species and further impacts electromigration of cations/anions. As predicted, the heavy metal/metal immigration under 15 mA is minimal and those under 35 mA and 50 mA are obvious, as shown in Figure 3. After extending the EDR duration longer than 4 h, the concentrations of Pb, Cd and Ni are below the detection limits and, thus, are not shown. The removal efficiencies of heavy metals/metals fluctuated under a current of 15 mA, especially for Al, Fe and Mg. The overall removal efficiency of heavy metals/metals under 15 mA was approximately 10%. An ionic current of 15 mA is mostly carried by protons (which can be validated by the constant pH) due to its nature of ultrafast transport [35]. For a current of 35 mA and 50 mA, the immigration of heavy metals/metals underwent a three-phase process, which was similar to previous studies [11]. The heavy metal/metal electromigration of soil fines, for instance, exhibited a four-phase changing tendency, which included a lag

phase, in which removal was substantially absent, a high removal rate, a low removal rate and a steady phase [11,36]. For this study, the absence of the lag phase occurred because the heavy metals/metals of ISSA acid extract were free and mobile in the anolyte and do not require acidification to be released from soils/ashes [11]. In addition, as shown in Figure 3c,e, a soft knee point of heavy metal/metal removal can be found from the beginning to 72 h in the EDR process, followed by a slow removal rate until 168 h, and then a steady rate afterwards. Except for Fe and Al, the EDR duration of 96 h can decrease the concentration of the total heavy metals/metals by approximately 75%, which is consistent with the prediction in the previous discussion.

Differences are observed in P concentration variation among these three currents. The P concentration under a current of 15 mA (Figure 3b) shows a continual increase due to the water consumption with the EDR process. At 35 mA and 50 mA (Figure 3d), the P concentration increases until 120 h and decreases afterwards. This is because intense currents prompt the transportation of positively charged P (such as $Ca(H_2PO_4)^+$) through CEM and immigrating to the catholyte, thereby resulting in the loss of P in the anolyte, which is consistent with previous studies [18].

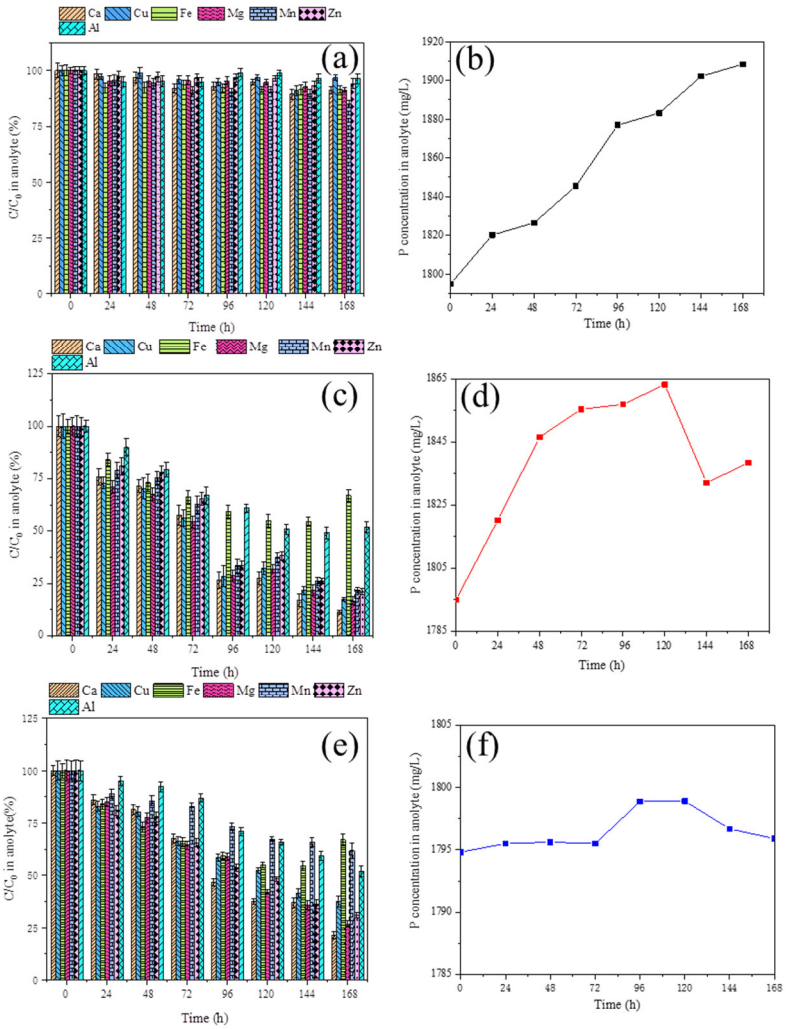

Figure 3. Residual percentage of heavy metals/metals in anolyte (current of 15 mA (**a**), 35 mA (**c**) and 50 mA (**e**)) and P concentration changes in anolyte (current of 15 mA (**b**), 35 mA (**d**) and 50 mA (**f**)).

3.3. Voltammetry and pH Variation

The pH changes and voltage variation of these two currents are shown in Figure 4. For a current of 15 mA (Figure 4a), the pH in the anolyte gradually decreases and slightly increases afterwards, which is due to the formation and immigration of H^+. The transferring of P species was dominantly determined by the H^+ concentration, as in our previous studies [9,37]. At pH 2, the P was dominantly in forms of $H_2PO_4^-$ and H_3PO_4 (their mass ratio was 1:1), while, at pH lower than 1, the P was dominantly in the form of H_3PO_4. Therefore, when pH of anolyte was lower than 1, the P was more easily escaping to anolyte with other cations. The pH in the catholyte is slightly increased due to the minimal formation of OH^- in the catholyte. For a current of 35 mA, the pH in anolyte kept dropping, while that in catholyte kept increasing and became alkaline after a duration of 48 h. However, for a current of 50 mA, the pH in the anolyte decreased until 48 h, and this decrease slowed down afterwards. In addition, in the catholyte, the pH during the first 24 h was obviously increased to approximately 14, and an inflexion appeared at 24 h, and then steadily increased afterwards. Consistently, visible precipitates gradually formed from 48 h. The low pH plateau in the 50 mA anolyte was consistent with the changes in the heavy metal/metal removal rate, resulting from the overflow of H^+ ions [38].

The voltage variations for 15 mA, 35 mA and 50 mA are shown in Figure 4d,e,f, respectively. There were two peaks for the voltage range of 15 mA, and these peaks were at 48 h and 72 h. The two climbing trends were indexed as the decreasing conductivity, which was caused by the formed H^+ that chelated with the negative ions (such as SO_4^{2-} and $H_2PO_4^-$). These two turning points may be due to the electromigration of cations from the anolyte to the catholyte, and the immigrated cations released H^+ in the catholyte and increased the conductivity of the system [39]. In addition, some slightly soluble salts (such as $Ca(OH)_2$) adhered to the CEM, causing a sharp rise in the EDR system [33]. The voltage of 35 mA shows a fast decreasing (0–24 h), a slower decreasing (24–72 h), and followed with a marginal decreasing (after 72 h). This process assists with the heavy metal variation process, which is caused by continually formed H^+ and OH^-. For a current of 50 mA, the cell voltage increased to a peak and decreased after 180 min. The high voltage at the beginning of the EDR process suggested that the heavy metal/metal removal efficiency was fast [38]. The following factors contributed to the decreasing overall cell voltage: first, the migration of heavy metals/metals from the anolyte to the catholyte and the formed precipitates; second, the change in cathodic and anodic overpotentials; and, third, the precipitates or deposits formed near the CEM [17,18,40]. The gradual decrease in cell voltage until 96 h verified that the EDR process of 96 h was the optimal heavy metal/metal removal time.

Thus, the current of 50 mA can effectively remove the heavy metals/metals from the P extract. With the extension of the EDR process, precipitates were formed, and the membrane pores were blocked, which caused the migration of ions to fall sharply; this was described as an "avalanche reaction" by Tanaka [41]. Therefore, it is necessary to optimize the EDR duration time. For further evaluating the economic parameters of this method, it is important to consider its energy consumption [42]. The general energy consumption and P-removal efficiency from heavy metals/metals with under a current of 50 mA and EDR durations of 96 h and 168 h are compared in Table 3. As shown, extending the EDR duration to 168 h doubled the energy consumption; however, the purity of the P extract was not improved accordingly. The efficiencies of removing Ca, Cu, Mg, Mn, Zn and Al elements were only improved by 15.18%, 10.93%, 12.03%, 11.94% and 8.97%, respectively. However, the removal efficiency of Fe was deceased by 7.65%, and the P was immigrated to catholyte by 3.67%. As such, in considering the energy efficiency and heavy metal/metal removal efficiency, 96 h was an optimal ED duration, which can achieve heavy metal/metal removal and prevent P loss.

Table 3. Element removal efficiency of 200 mL P extract for 96 h and 168 h under 50 mA and energy consumptions.

ED Duration (h)	Energy Consumption (KW.h)	Element Removal Efficiency (%)							
		Ca	Cu	Fe	Mg	Mn	Zn	Al	P
96	0.05	73.43	71.62	40.67	71.26	66.72	66.32	39.16	0
168	0.11	88.61	82.55	33.02	83.29	78.26	79.05	48.13	3.62

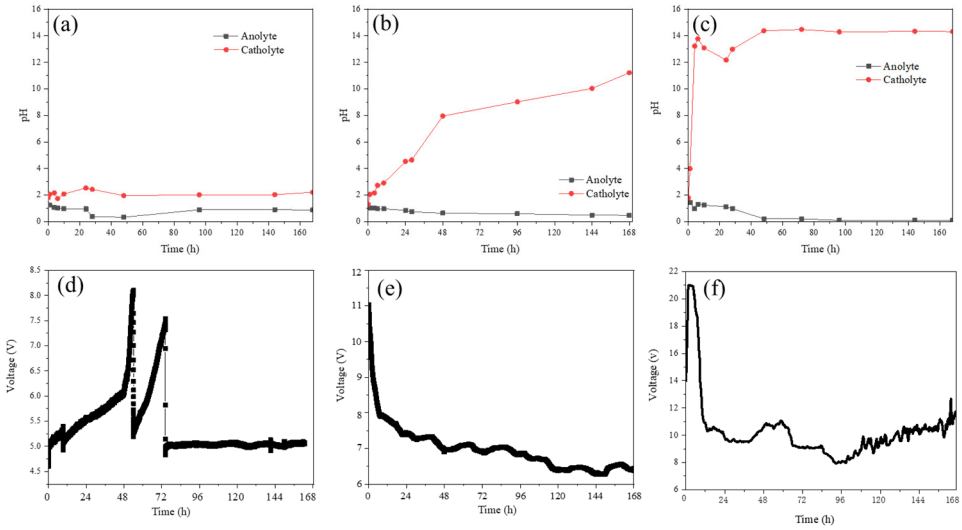

Figure 4. pH changes in anolyte and catholyte of 15 mA (**a**), 35 mA (**b**) and 50 mA (**c**) and voltage variation of 15 mA (**d**), 35 mA (**e**) and 50 mA (**f**).

3.4. Precipitates in Catholyte

To recover more precipitates, this ED process under 50 mA was ended at 14 days. At the end of the ED process, the volume of anolyte was decreased to 95 mL and that of the catholyte was approximately 120 mL because of the water splitting that occurred in the anolyte and catholyte. In addition, the dehydration mechanism could be explained by the following aspects: charge capillary column theory and ionic potential [43,44].

The flocculent precipitates in the catholyte grew dense and gathered into two kinds of precipitates, which were precipitate 1 (yellow color) and precipitate 2 (white color). This is because the alkaline nature of the catholyte caused some metals/heavy metals to precipitate after being transferred from the anolyte into the catholyte.

With the extension of electrolysis time, in addition to heavy metals/metals, P was gradually transferred into the catholyte, especially after 7 days, as shown in Figure 5. After 14 days of the EDR process, the concentrations of heavy metals, metals and P decreased significantly in the anolyte and increased in the catholyte, as shown in Table 4. The final pH of the anolyte was approximately 0.087, while that of the catholyte was 14.31. The acidification of the anolyte forms positively charged metal-P complexes, such as $Fe(H_2PO_4)^{2+}$ and $Al(H_2PO_4)^{2+}$, which causes P migration to the catholyte [18]. Considering the volume decrease in the anolyte, the amount of P in the anolyte was decreased by approximately 11.11%.

Table 4. Contents of anolyte and catholyte after the EDR process (50 mA, 14 days).

Electrolyte	pH	Concentration of Major Metal(loid)s (mg/L)	Concentration of Minor Metal(loid)s (μg/L)
Anolyte	0.087	Ca (822.22), P (1701), Al (718.30), Mg (2.65), Fe (4.26), Zn (0.36), Cu (0.13), Mn (0.09).	As (5.16), Ni (10.8), Pb (5.12).
Catholyte	14.31	Ca (322.22), P (309), Al (418.30), Mg (0.65), Fe (0.16), Zn (0.06).	As (1.87), Ni (3.28), Pb (1.98).

Through the XRD results (Figure 6), it was identified that these two kinds of precipitates were poorly crystallized and were present mainly in the form of $Ca_5(PO_4)_3(OH)$, Ca_3SiO_5 and $Ca_2(SiO_4)$. The microstructure of these two precipitates can be found in Figure 7. Precipitate 1 was a snowflake and precipitate 2 was loosely spherical. The major contents of these two precipitates were further identified, and detailed element mapping (Al and P) can be found in Figure 8. The difference in color of these two precipitates may be because of the different contents of Fe, which were 0.22% in precipitate 1 (yellow color) and 0.04% in precipitate 2 (white color). The assembly of transformed P was greater in precipitate 1, while more Al was assembled in precipitate 2.

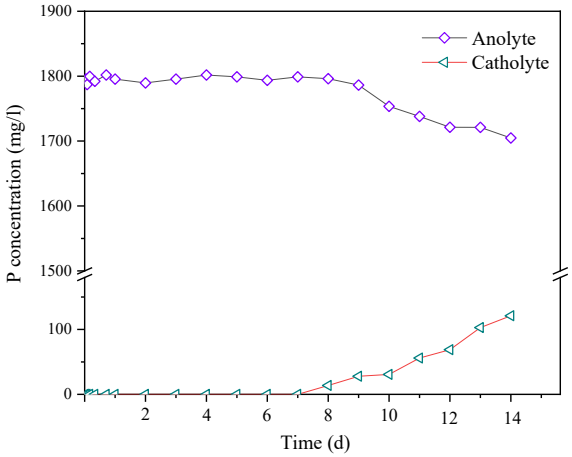

Figure 5. P transformation (mg/L) from anolyte to catholyte.

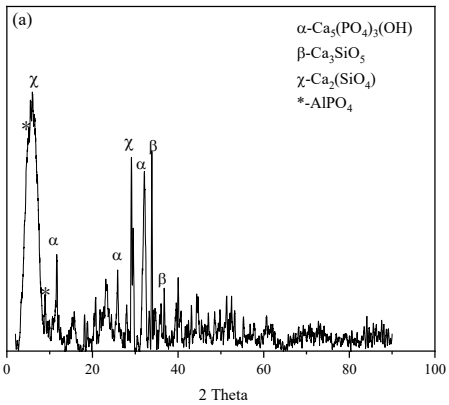

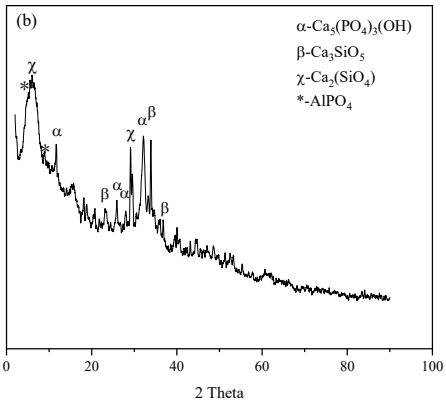

Figure 6. XRD of two kinds of precipitates in catholyte ((**a**), precipitate 1, (**b**), precipitate 2). (Reference codes of $Ca_5(PO_4)_3(OH)$, Ca_3SiO_5, $Ca_2(SiO_4)$ and $AlPO_4$ were 01-086-0740, 00-016-0406, 01-087-1258, and 01-088-1680, respectively.).

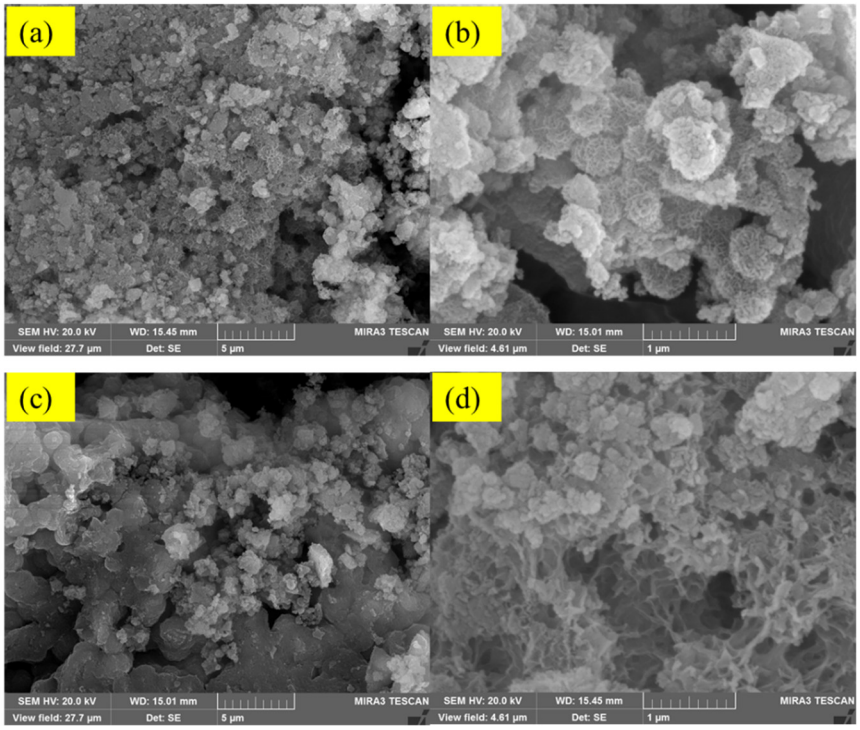

Figure 7. SEM of two kinds of precipitates ((**a**,**b**) are precipitate 1, (**c**,**d**) are precipitate 2).

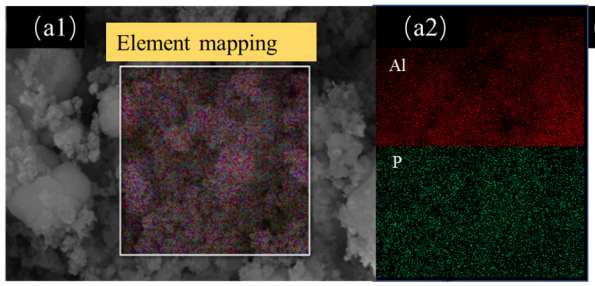

Elements	Atomic percentage (%)
C	21.74
O	58.54
Na	1.96
Mg	2.33
Al	10.03
Si	0.77
P	2.19
S	0.55
K	0.29
Ca	1.26
Fe	0.22
Zn	0.12

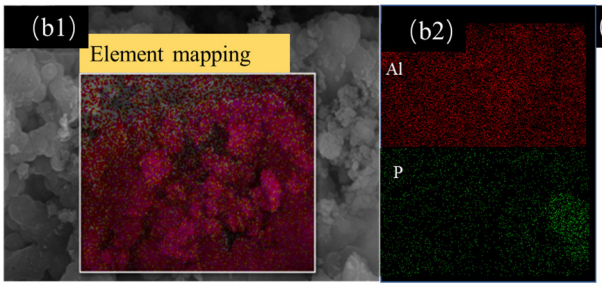

Elements	Atomic percentage (%)
C	19.25
O	59.12
Na	0.75
Mg	1.02
Al	18.08
P	0.80
S	0.25
Cl	0.09
K	0.07
Ca	0.47
Fe	0.04
Zn	0.07

Figure 8. Element mapping (**a1** and **a2** were precipitate 1; **b1** and **b2** were precipitate 2) and EDS (**a3**, precipitate 1; **b3**, precipitate 2) of two kinds of precipitates.

4. Conclusions

Combining the acid extract and electrodialytic remediation can shorten the electrodialytic time, save energy, prevent the problem of membrane blockage and increase the P extraction and purification efficiency. An electrodialytic remediation time of 96 h under a constant electricity of 50 mA can mostly remove major heavy metals/metals, including Ca (73.43%), Cu (71.62%), Mg (71.26%), Mn (66.72%) and Zn (66.32%). For Al, Fe and As, their removal efficiency was very low because of their low charge and large hydrated ionic radius. P was lost as the electrodialytic process extended (especially after 96 h). Extending the ED process to 14 days did not significantly remove the heavy metals/metals. In contrast, this process doubles the energy consumption and causes P to become lost in the anolyte. The immigrated P can be precipitated with Al and Ca and form flocculent precipitates. In addition, these precipitates were gathered in two kinds of precipitates (precipitate 1, yellow color, and precipitate 2, white color), and the P was more condensed in precipitate 1 and in the form of $Ca_5(PO_4)_3(OH)$. The recovered P in precipitate 1 had a relatively high purity, which was also a secondary P recovery route.

Author Contributions: Conceptualization, L.F.; methodology, L.F.; software, L.F.; validation, Y.M., L.X. and Z.R.; formal analysis, L.F.; investigation, L.F.; resources, L.F.; data curation, L.F.; writing—original draft preparation, L.F.; writing—review and editing, L.F.; visualization, L.F.; supervision, Z.Z.; project administration, L.F.; funding acquisition, L.F. All authors have read and agreed to the published version of the manuscript.

Funding: The Major Scientific and Technological Innovation Projects of Shandong Province (2021CXGC011201), National Natural Science Foundation of China (No. 52200142), and the start-up funding for the newly introduced talents at Beijing Normal University (28707-111032107).

Acknowledgments: The authors would like to thank the Major Scientific and Technological Innovation Projects of Shandong Province (2021CXGC011201) for their support, National Natural Science Foundation of China (No. 52200142), and the start-up funding for the newly introduced talents at Beijing Normal University (28707-111032107).

Conflicts of Interest: The authors declare no conflict of interest.

References

1. Kirkelund, G.M.; Magro, C.; Guedes, P.; Jensen, P.E.; Ribeiro, A.B.; Ottosen, L.M. Electrodialytic removal of heavy metals and chloride from municipal solid waste incineration fly ash and air pollution control residue in suspension—Test of a new two compartment experimental cell. *Electrochim. Acta* **2015**, *181*, 73–81. https://doi.org/10.1016/j.electacta.2015.03.192.
2. Donatello, S.; Cheeseman, C.R. Recycling and recovery routes for incinerated sewage sludge ash (ISSA): A review. *Waste Manag.* **2013**, *33*, 2328–2340.
3. Petzet, S.; Peplinski, B.; Bodkhe, S.Y.; Cornel, P. Recovery of phosphorus and aluminium from sewage sludge ash by a new wet chemical elution process (SESAL-Phos-recovery process). *Water Sci. Technol.* **2011**, *64*, 693–699.
4. Franz, M. Phosphate fertilizer from sewage sludge ash (SSA). *Waste Manag.* **2008**, *28*, 1809–1818.
5. Fytili, D.; Zabaniotou, A. Utilization of sewage sludge in EU application of old and new methods—A review. *Renew. Sustain. Energy Rev.* **2008**, *12*, 116–140. https://doi.org/10.1016/j.rser.2006.05.014.
6. Herzel, H.; Krüger, O.; Hermann, L.; Adam, C. Sewage sludge ash—A promising secondary phosphorus source for fertilizer production. *Sci. Total Environ.* **2016**, *542*, 1136–1143. https://doi.org/10.1016/j.scitotenv.2015.08.059.
7. Adam, C.; Peplinski, B.; Michaelis, M.; Kley, G.; Simon, F.G. Thermochemical treatment of sewage sludge ashes for phosphorus recovery. *Waste Manag.* **2009**, *29*, 1122–1128. https://doi.org/10.1016/j.wasman.2008.09.011.
8. Petzet, S.; Peplinski, B.; Cornel, P. On wet chemical phosphorus recovery from sewage sludge ash by acidic or alkaline leaching and an optimized combination of both. *Water Res.* **2012**, *46*, 3769–3780. https://doi.org/10.1016/j.watres.2012.03.068.
9. Fang, L.; Li, J.S.; Guo, M.Z.; Cheeseman, C.R.; Tsang, D.C.W.; Donatello, S.; Poon, C.S. Phosphorus recovery and leaching of trace elements from incinerated sewage sludge ash (ISSA). *Chemosphere* **2018**, *193*, 278–287. https://doi.org/10.1016/j.chemosphere.2017.11.023.
10. Pedersen, K.B.; Ottosen, L.M.; Jensen, P.E.; Lejon, T. Comparison of 2-compartment, 3-compartment and stack designs for electrodialytic removal of heavy metals from harbour sediments. *Electrochim. Acta* **2015**, *181*, 48–57. https://doi.org/10.1016/j.electacta.2014.12.003.
11. Ottosen, L.M.; Jensen, P.E.; Kirkelund, G.M. Phosphorous recovery from sewage sludge ash suspended in water in a two-compartment electrodialytic cell. *Waste Manag.* **2016**, *51*, 142–148. https://doi.org/10.1016/j.wasman.2016.02.015.
12. Ebbers, B.; Ottosen, L.M.; Jensen, P.E. Comparison of two different electrodialytic cells for separation of phosphorus and heavy metals from sewage sludge ash. *Chemosphere* **2015**, *125*, 122–129. https://doi.org/10.1016/j.chemosphere.2014.12.013.
13. Fournie, T.; Rashwan, T.L.; Switzer, C.; Gerhard, J.I. Phosphorus recovery and reuse potential from smouldered sewage sludge ash. *Waste Manag.* **2022**, *137*, 241–252. https://doi.org/10.1016/j.wasman.2021.11.001.
14. Luyckx, L.; Caneghem, J.V. Recovery of phosphorus from sewage sludge ash: Influence of chemical addition prior to incineration on ash mineralogy and related phosphorus and heavy metal extraction. *J. Environ. Chem. Eng.* **2022**, *10*, 108117. https://doi.org/10.1016/j.jece.2022.108117.
15. Yu, X.; Nakamura, Y.; Otsuka, M.; Omori, D.; Haruta, S. Development of a novel phosphorus recovery system using incinerated sewage sludge ash (ISSA) and phosphorus-selective adsorbent. *Waste Manag.* **2021**, *120*, 41–49. https://doi.org/10.1016/j.wasman.2020.11.017.
16. Wang, Q.; Li, J.-S.; Xue, Q.; Poon, C.S. Alkaline modification of the acid residue of incinerated sewage sludge ash after phosphorus recovery for heavy metal removal from aqueous solutions. *Waste Manag.* **2021**, *123*, 80–87. https://doi.org/10.1016/j.wasman.2021.01.025.
17. Guedes, P.; Couto, N.; Ottosen, L.M.; Ribeiro, A.B. Phosphorus recovery from sewage sludge ash through an electrodialytic process. *Waste Manag.* **2014**, *34*, 886–892. https://doi.org/10.1016/j.wasman.2014.02.021.
18. Viader, R.P.; Jensen, P.E.; Ottosen, L.M.; Ahrenfeldt, J.; Hauggaard-Nielsen, H. Electrodialytic extraction of phosphorus from ash of low-temperature gasification of sewage sludge. *Electrochim. Acta* **2015**, *181*, 100–108. https://doi.org/10.1016/j.electacta.2015.05.025.
19. Pedersen, K.B.; Lejon, T.; Jensen, P.E.; Ottosen, L.M. Applying multivariate analysis as decision tool for evaluating sediment-specific remediation strategies. *Chemosphere* **2016**, *151*, 59–67. https://doi.org/10.1016/j.chemosphere.2016.02.063.
20. Kirkelund, G.M.; Ottosen, L.M.; Villumsen, A. Investigations of Cu, Pb and Zn partitioning by sequential extraction in harbour sediments after electrodialytic remediation. *Chemosphere* **2010**, *79*, 997–1002. https://doi.org/10.1016/j.chemosphere.2010.03.015.
21. Lafi, R.; Gzara, L.; Lajimi, R.H.; Hafiane, A. Treatment of textile wastewater by a hybrid ultrafiltration/electrodialysis process. *Chem. Eng. Process. Process Intensif.* **2018**, *132*, 105–113. https://doi.org/10.1016/j.cep.2018.08.010.
22. Al Aji, B.; Yavuz, Y.; Koparal, A.S. Electrocoagulation of heavy metals containing model wastewater using monopolar iron electrodes. *Sep. Purif. Technol.* **2012**, *86*, 248–254. https://doi.org/10.1016/j.seppur.2011.11.011.
23. Wang, J.W.; Bejan, D.; Bunce, N.J. Removal of arsenic from synthetic acid mine drainage by electrochemical pH adjustment and coprecipitation with iron hydroxide. *Environ. Sci. Technol.* **2003**, *37*, 4500–4506. https://doi.org/10.1021/es030359y.
24. Sadyrbaeva, T.Z. Removal of chromium(VI) from aqueous solutions using a novel hybrid liquid membrane—Electrodialysis process. *Chem. Eng. Process. Process Intensif.* **2016**, *99*, 183–191. https://doi.org/10.1016/j.cep.2015.07.011.
25. Sun, T.R.; Ottosen, L.M.; Jensen, P.E.; Kirkelund, G.M. Effect of pulse current on acidification and removal of Cu, Cd, and As during suspended electrodialytic soil remediation. *Electrochim. Acta* **2013**, *107*, 187–193. https://doi.org/10.1016/j.electacta.2013.05.138.
26. Pedersen, K.B.; Jensen, P.E.; Ottosen, L.M.; Lejon, T. An optimised method for electrodialytic removal of heavy metals from harbour sediments. *Electrochim. Acta* **2015**, *173*, 432–439. https://doi.org/10.1016/j.electacta.2015.05.050.

27. Chen, W.; Jensen, P.E.; Ottosen, L.M.; Kirkelund, G.M. Electrodialytic remediation of fly ash from co-combustion of wood and straw. *Electrochim. Acta* **2015**, *181*, 208–216. https://doi.org/10.1016/j.electacta.2015.04.083.
28. Ilhan, F.; Kabuk, H.A.; Kurt, U.; Avsar, Y.; Sari, H.; Gonullu, M.T. Evaluation of treatment and recovery of leachate by bipolar membrane electrodialysis process. *Chem. Eng. Process. Process Intensif.* **2014**, *75*, 67–74. https://doi.org/10.1016/j.cep.2013.11.005.
29. Ottosen, L.M.; Jensen, P.E.; Kirkelund, G.M. Electrodialytic Separation of Phosphorus and Heavy Metals from Two Types of Sewage Sludge Ash. *Sep. Sci. Technol.* **2014**, *49*, 1910–1920. https://doi.org/10.1080/01496395.2014.904347.
30. Fang, L.; Li, J.-S.; Donatello, S.; Cheeseman, C.R.; Wang, Q.; Poon, C.S.; Tsang, D.C.W. Recovery of phosphorus from incinerated sewage sludge ash by combined two-step extraction and selective precipitation. *Chem. Eng. J.* **2018**, *348*, 74–83. https://doi.org/10.1016/j.cej.2018.04.201.
31. Liang, S.; Yang, L.; Chen, H.; Yu, W.; Tao, S.; Yuan, S.; Xiao, K.; Hu, J.; Hou, H.; Liu, B.; et al. Phosphorus recovery from incinerated sewage sludge ash (ISSA) and reutilization of residues for sludge pretreated by different conditioners. *Resour. Conserv. Recycl.* **2021**, *169*, 105524. https://doi.org/10.1016/j.resconrec.2021.105524.
32. Yuan, L.Z.; Xu, X.J.; Li, H.Y.; Wang, N.N.; Guo, N.; Yu, H.W. Development of novel assisting agents for the electrokinetic remediation of heavy metal-contaminated kaolin. *Electrochim. Acta* **2016**, *218*, 140–148. https://doi.org/10.1016/j.electacta.2016.09.121.
33. Chen, Q.B.; Ji, Z.Y.; Liu, J.; Zhao, Y.Y.; Wang, S.Z.; Yuan, J.S. Development of recovering lithium from brines by selective-electrodialysis: Effect of coexisting cations on the migration of lithium. *J. Membr. Sci.* **2018**, *548*, 408–420. https://doi.org/10.1016/j.memsci.2017.11.040.
34. Park, H.B.; Kamcev, J.; Robeson, L.M.; Elimelech, M.; Freeman, B.D. Maximizing the right stuff: The trade-off between membrane permeability and selectivity. *Science* **2017**, *356*, eaab0530. https://doi.org/10.1126/science.aab0530.
35. Hassanali, A.; Giberti, F.; Cuny, J.; Kuhne, T.D.; Parrinello, M. Proton transfer through the water gossamer. *Proc. Natl. Acad. Sci. USA* **2013**, *110*, 13723–13728. https://doi.org/10.1073/pnas.1306642110.
36. Pedersen, K.B.; Lejon, T.; Jensen, P.E.; Ottosen, L.M. The influence of sediment properties and experimental variables on the efficiency of electrodialytic removal of metals from sediment. *J. Environ. Chem. Eng.* **2017**, *5*, 5312–5321. https://doi.org/10.1016/j.jece.2017.10.031.
37. Fang, L.; Li, J.-S.; Donatello, S.; Cheeseman, C.R.; Poon, C.S.; Tsang, D.C.W. Use of Mg/Ca modified biochars to take up phosphorus from acid-extract of incinerated sewage sludge ash (ISSA) for fertilizer application. *J. Clean. Prod.* **2020**, *244*, 118853. https://doi.org/10.1016/j.jclepro.2019.118853.
38. Jensen, P.E.; Ottosen, L.M.; Ferreira, C.; Villumsen, A. Kinetics of electrodialytic extraction of Pb and soil cations from a slurry of contaminated soil fines. *J. Hazard. Mater.* **2006**, *138*, 493–499. https://doi.org/10.1016/j.jhazmat.2006.05.073.
39. Daud, S.M.; Daud, W.R.W.; Kim, B.H.; Somalu, M.R.; Abu Bakar, M.H.; Muchtar, A.; Jahim, J.M.; Lim, S.S.; Chang, I.S. Comparison of performance and ionic concentration gradient of two-chamber microbial fuel cell using ceramic membrane (CM) and cation exchange membrane (CEM) as separators. *Electrochim. Acta* **2018**, *259*, 365–376. https://doi.org/10.1016/j.electacta.2017.10.118.
40. Sun, T.R.; Ottosen, L.M.; Mortensen, J. Electrodialytic soil remediation enhanced by low frequency pulse current—Overall chronopotentiometric measurement. *Chemosphere* **2013**, *90*, 1520–1525. https://doi.org/10.1016/j.chemosphere.2012.08.038.
41. Tanaka, Y.; Seno, M. Concentration Polarization and Water Dissociation in Ion-Exchange Membrane Electrodialysis—Mechanism of Water Dissociation. *J. Chem. Soc. -Faraday Trans. I* **1986**, *82*, 2065–2077. https://doi.org/10.1039/f19868202065.
42. Shrestha, R.; Ban, S.; Devkota, S.; Sharma, S.; Joshi, R.; Tiwari, A.P.; Kim, H.Y.; Joshi, M.K. Technological trends in heavy metals removal from industrial wastewater: A review. *J. Environ. Chem. Eng.* **2021**, *9*, 105688. https://doi.org/10.1016/j.jece.2021.105688.
43. Jiang, C.X.; Wang, Q.Y.; Li, Y.; Wang, Y.M.; Xu, T.W. Water electro-transport with hydrated cations in electrodialysis. *Desalination* **2015**, *365*, 204–212. https://doi.org/10.1016/j.desal.2015.03.007.
44. Eisenman, G. Cation selective glass electrodes and their mode of operation. *Biophys. J.* **1962**, *2*, 259–323.